

Automated optimization of TMS coil placement for personalized functional network engagement

Charles J. Lynch, Immanuel Elbau, Tommy H. Ng, Danielle Wolk, Shasha Zhu, Aliza Ayaz, Jonathan D. Power, Benjamin Zebley, Faith M. Gunning, Conor Liston

Supplemental Materials

Figure S1. Reliable functional network mapping can be obtained with smaller, clinically-tractable quantities of multi-echo fMRI data, Related to Figure 1. The analyses reported in the main text involved mapping functional networks using each patient's entire resting-state multi-echo fMRI dataset (up to 29.86 hours per-patient). We asked if similar functional network maps could be obtained in each individual when using smaller, more clinically-tractable quantities of data. To address this question, functional networks were re-mapped using contiguous subsets of each individual's full dataset (starting with their first 14.5 minute scan and increasing in single scan increments). The adjusted Rand coefficient was used to measure the similarity (the fraction of node pairs identified in the same way after correcting for chance, higher values indicating higher similarity) of functional network maps derived from a subset and the full dataset. (A) Data quantity x similarity curves for each individual (both depressed and non-depressed, except for ME06, who only had 2 x 14.5 minute scans from a single study visit) are shown as gray lines. The red line represents the average adjusted Rand coefficient for the 13 individuals included in this analysis. On average, the adjusted Rand coefficient increased rapidly with data quantity initially but plateaued approximately around 120 minutes. (B) Difference in adjusted Rand values associated with a single 14.5 minute scan when analyzed as a multi-echo and "pseudo" single-echo dataset (the latter obtained by using only the second echo, as done in (Lynch et al., 2020)). (C) Representative examples of functional networks mapped in 2 patients (MD01 and MD04) and 1 healthy individual (ME01) when using the first 14.5-, 29-, and 116-minutes of (multi-echo) data versus the full dataset. (D) Targeting the same area of the left dorsolateral prefrontal cortex likely stimulates different sets of functional brain networks in 5 healthy, non-depressed individuals. Functional brain networks were mapped in each healthy individual using their entire resting-state fMRI dataset. Results from two representative individuals (ME01 and ME02) are shown. (E) The electric field (E-field) generated by the TMS coil set directly over the MNI coordinates X=-42, Y=44, Z=30 transformed in the native image space (F) The E-field hotspot is operationalized using percentile based thresholds (99% to 99.9%, in 0.1% steps). (G) Variability in functional network stimulation in the 6 non-depressed individuals summarized in a horizontal stacked bar graph.

Figure S1

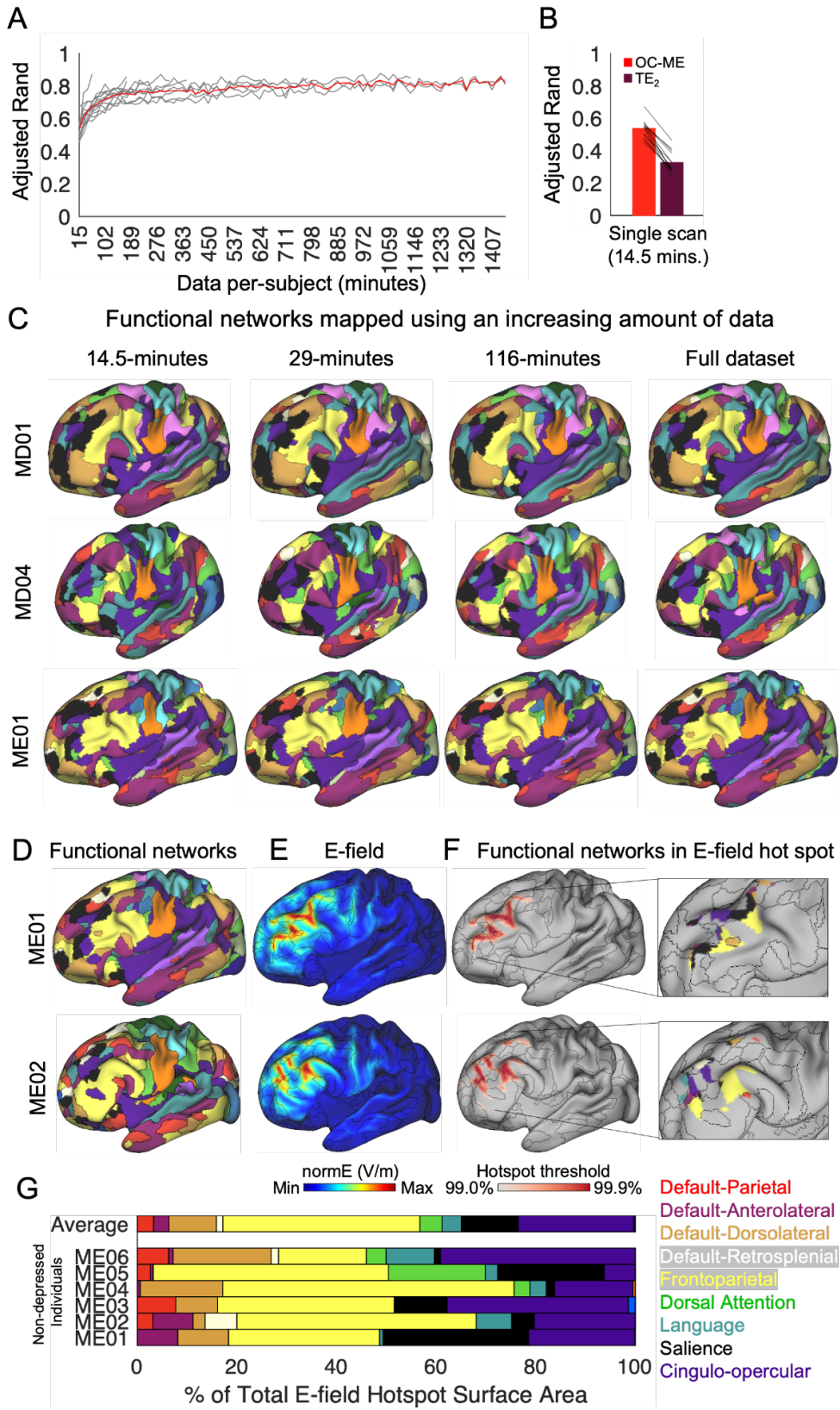


Figure S2. Effect of cortical folding and stimulation intensity on the spatial distribution of the E-field produced by TMS, Related to Figure 2. The electric field (E-field) produced by a TMS pulse is strongest on the gyral crown (Bungert et al., 2017; Siebner et al., 2022; Thielscher et al., 2011). For this reason, achieving selective stimulation of a network cluster located in a sulcus is not possible, because the nearest gyral crown will always receive a greater level of stimulation. (A) Sulcal map (red = gyrus, blue = sulcus) displayed on four representative patient's pial and inflated cortical surface. (B) The E-field hotspot displayed on the patient's pial and inflated cortical surface. A complex and multifocal stimulation pattern is revealed when visualizing the E-field hotspot on the inflated surface. (C) The strength of the E-field varies linearly with dI/dt (the speed of variation of the current throughout the coil) and, for this reason, does not change its spatial distribution. This effect is shown in MD02 where, as the stimulation intensity increases (in this hypothetical case, from $dI/dt = 1 \text{ A}/\mu\text{s}$ to $155 \text{ A}/\mu\text{s}$, which corresponds approximately the possible range of realized dI/dt on our MagPro X100 machine when using the B70 coil), the spatial distribution of the E-field remains the same (including where the E-field is maximal, or the "hotspot").

Figure S2

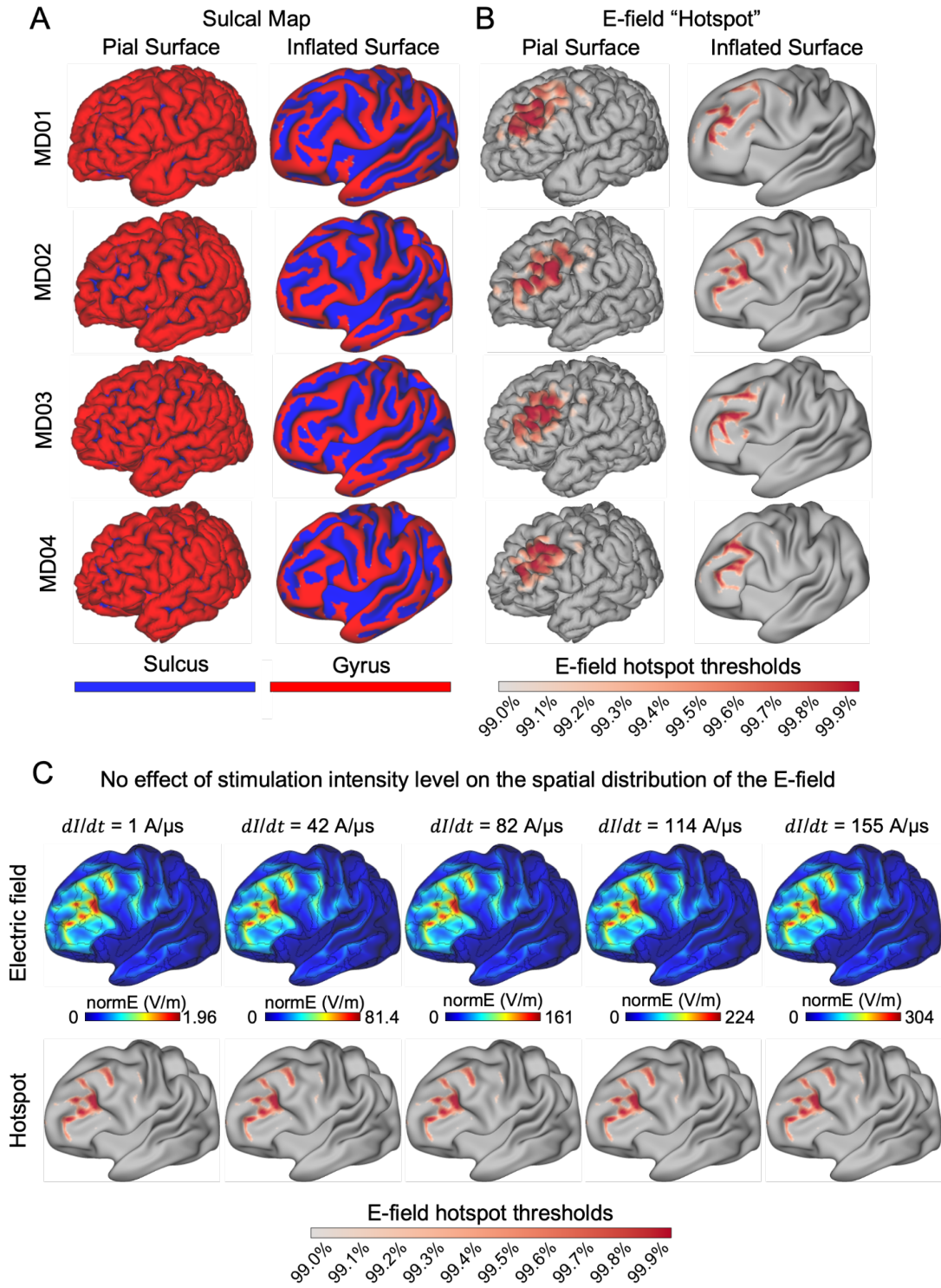


Figure S3. Variability in stimulation specificity achieved by TANS is related to differences in network size across individuals, Related to Figure 3. (A) The optimal coil placement found by the Targeted Functional Network Stimulation (“TANS”) approach for stimulating the frontoparietal network in two representative non-depressed individuals (ME01 and ME02). Circular heatmaps describe how the on-target value changes with the coil orientation (the coil orientation displayed is the one that maximized the on-target value). (B) The E-field associated with the optimal coil placement and boundaries of the target functional network (black borders). (C) Functional networks in the E-field hotspot (the 99.5% hotspot threshold is used for visualization purposes). (D) A stacked horizontal bar plot summarizes the percentage of the total E-field hotspot surface area that is occupied by each functional brain network. (E) The size of the target network cluster was positively correlated ($r = 0.75$, $p = 0.002$) with the on-target value achieved by TANS, suggesting that larger networks were more likely to be stimulated with minimal off-target effects than smaller ones. For example, very little (approximately 500 mm²) of the frontoparietal network was accessible in MD08 and consequently the on-target value achieved by TANS was relatively low (55% of E-field hotspot occupied by frontoparietal network). In contrast, in MD06, the frontoparietal network patch was larger and the on-target value achieved was relatively high (93% of E-field hotspot occupied by frontoparietal network).

Figure S3

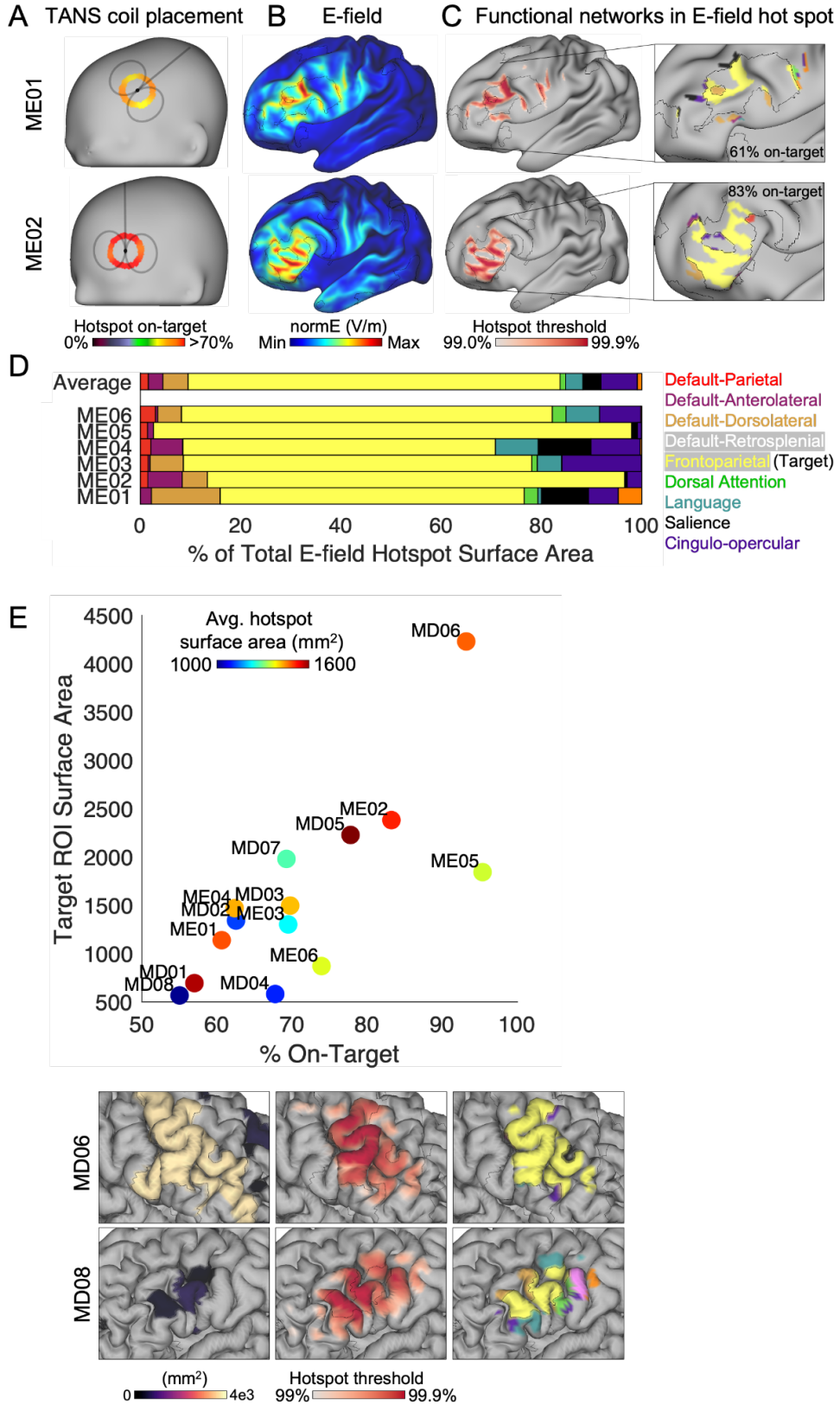


Figure S4. **Comparing the performance of TANS in silico to two other targeting approaches in 6 healthy, non-depressed individuals**, Related to Figure 4. Variability in functional brain network stimulation when using a generic (A), ADM (B), and TANS (C) coil placement. The relative improvement in the on-target value (the proportion of the E-field hotspot aligned with the frontoparietal network) within each individual (D). ADM = auxiliary dipole method, TANS = targeted functional network stimulation.

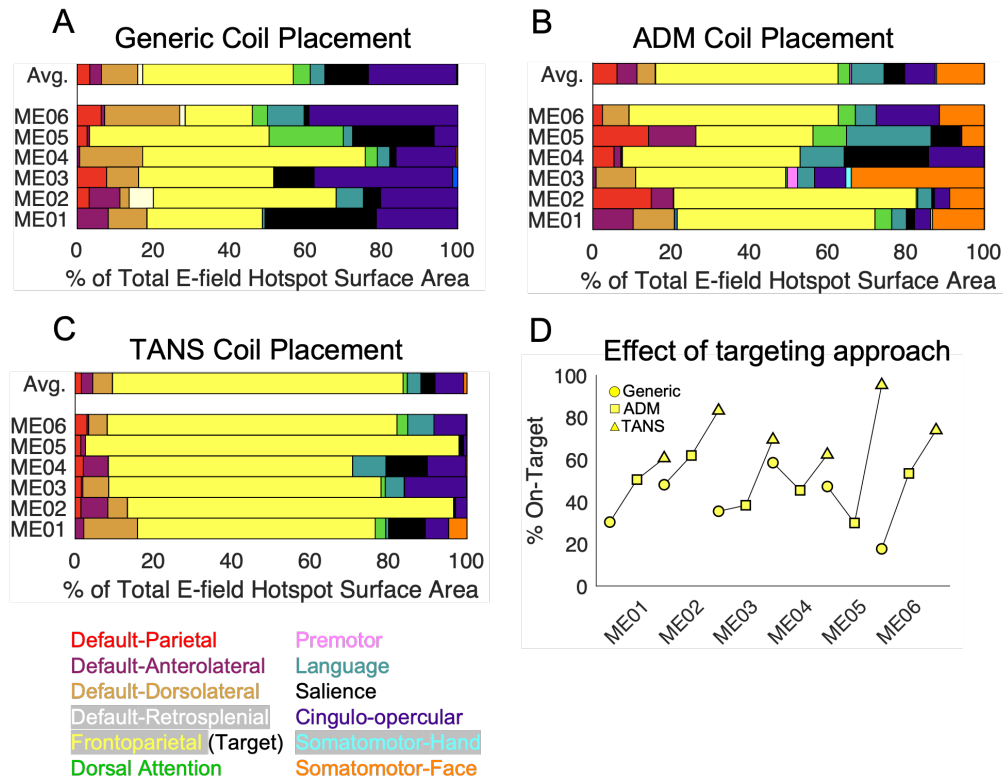


Figure S5. **The TANS approach increases the total amount of stimulation delivered to the target network**, Related to Figure 5. (A) The average E-field strength inside a 5mm ROI sphere set at the centroid of the target network cluster when using ADM. Square = ADM, Triangle = TANS. (B) E-field associated with the optimal coil placements identified by ADM (left) and TANS (right). Black borders represent the boundaries of the target functional network. Black arrows highlight stimulation extraneous to the target functional network when using ADM. (C) Total on-target and off-target stimulation (the sum V/m for all target and non-target network vertices inside the E-field hotspot) is shown for each individual. ADM = auxiliary dipole method, TANS = targeted functional network stimulation.

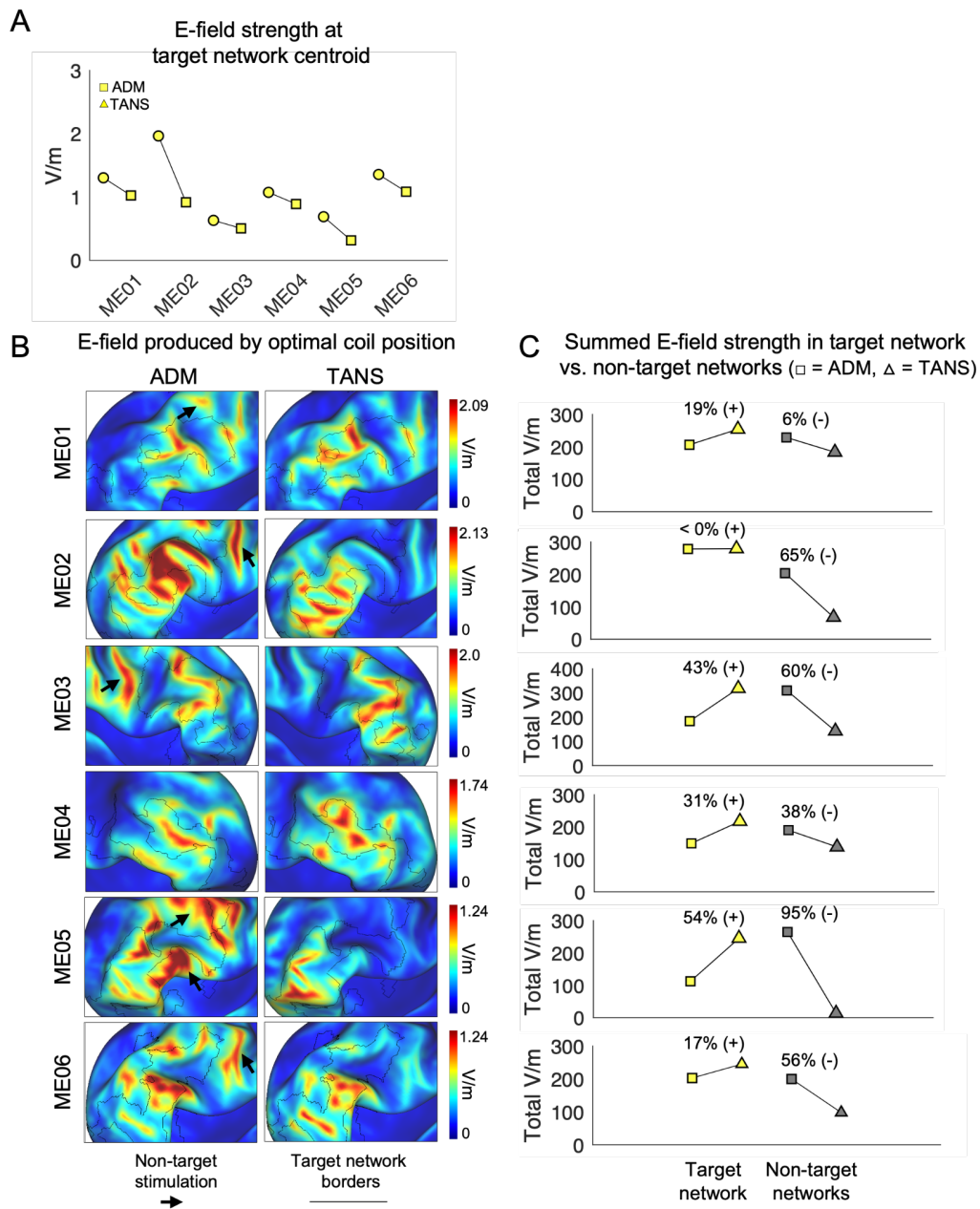


Figure S6. Evaluating the effect of stimulation intensity on stimulation specificity achieved in silico when using TANS versus two other targeting approaches in non-depressed individuals, Related to Figure 6. Two hypothetical neural activation thresholds are considered here, 100 V/m (left column) and 50 V/m (right column), for the generic (A), ADM (B), and TANS (C) coil placements. A range of stimulation intensities are considered (from $dl/dt = 1 \text{ A}/\mu\text{s}$ to $155 \text{ A}/\mu\text{s}$, which corresponds approximately to the possible range of realized dl/dt on our MagPro X100 machine when using the B70 coil). The relative improvement in the on-target value (the maximum proportion of the suprathreshold E-field hotspot that is aligned with the frontoparietal network) within each individual (D). The unique colors represent different study participants. TANS = targeted functional network stimulation, ADM = auxiliary dipole method. Circle = Generic, Square = ADM, Triangle = TANS.

Figure S6

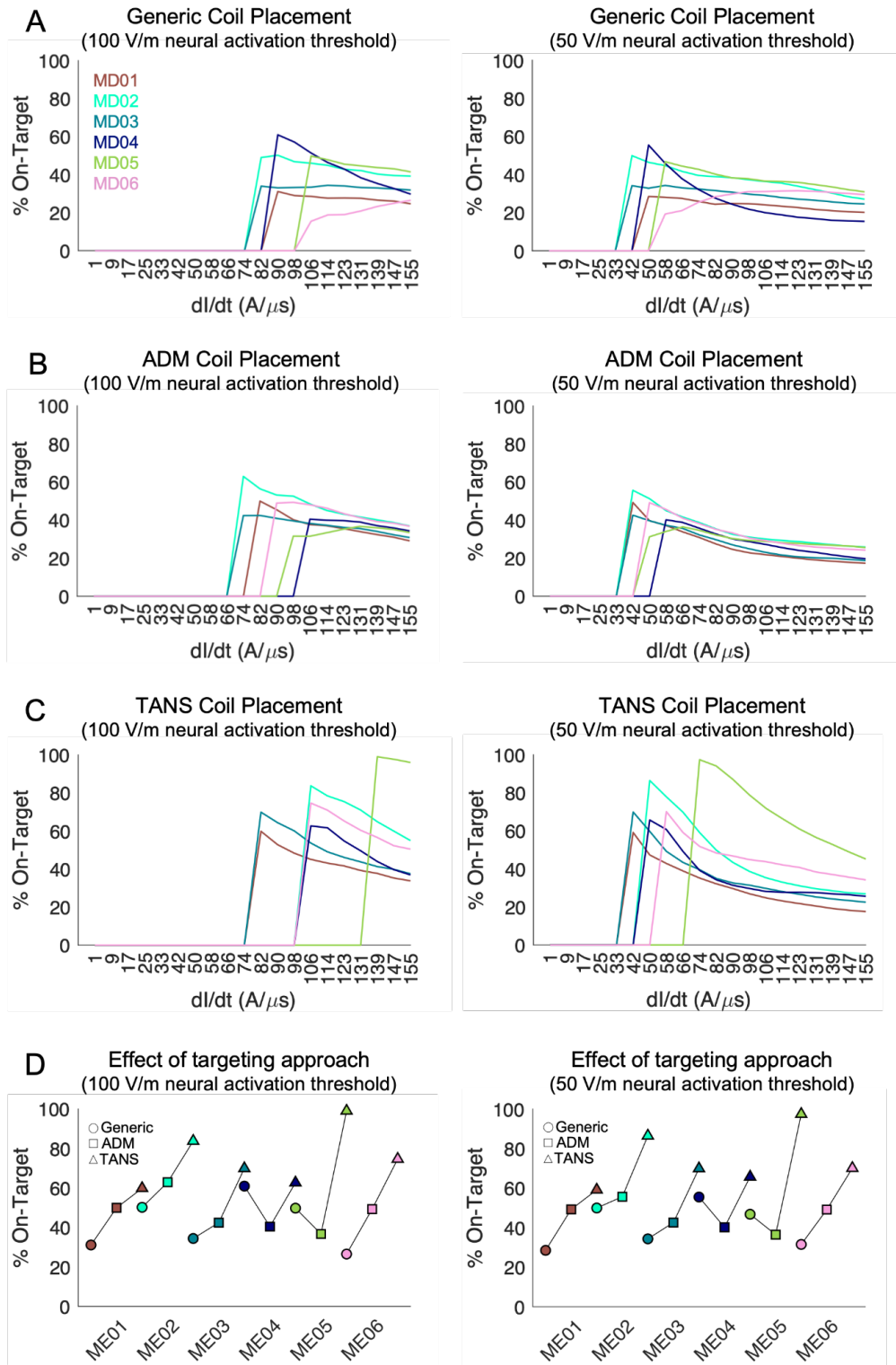


Figure S7. **Replication of the motor cortex validation experiment in two additional healthy individuals**, Related to Figure 7. (A) The somatomotor-foot (dark green), somatomotor-hand (cyan), and somatomotor-face (tan) functional networks in ME02 and ME06. (B) The E-fields associated with the ADM and TANS coil placements for both the somatomotor-foot (top row) and somatomotor-hand (bottom row) targets in ME02. White arrows highlight inadvertent stimulation of the somatomotor-hand network when using ADM to target the somatomotor-foot network. (C-D) The total amount of on-target and off-target stimulation (the sum V/m for all target and non-target network vertices inside the E-field hotspot) is increased and decreased, respectively, when using TANS when compared to ADM in ME02 (C), and to a lesser extent in ME06 (D). All simulations were performed with the stimulation intensity set to $dl/dt = 1 \text{ A}/\mu\text{s}$. (E-F) The percentage of single TMS pulses (stimulation intensity ranging from 35% to 80% of MSO, in 5% steps) delivered to somatomotor-foot and somatomotor-hand networks in ME02 (E) and ME06 (F) that produced a muscle contraction in either the contralateral lower (dark green) or upper limb (cyan). (E) In ME02, when targeting the somatomotor-foot network (top row of **Figure S7E**), only TANS elicited MEPs in the contralateral lower limb, whereas the ADM actually elicited MEPs in the contralateral upper limb (indicative of an off-target effect) and did not produce a foot MEP at any stimulation intensity level (hence the absence of green bars in the upper left panel). TANS and ADM both elicited muscle contractions in the target upper limb at the same stimulation intensity level (55% MSO) when targeting the somatomotor-hand network (bottom row of **Figure S7E**). (F) In ME06, TANS achieved muscle contractions at lower stimulation intensities than ADM for both the somatomotor-hand (40% MSO vs. 55% MSO) and somatomotor-foot (65% vs. 70% MSO) targets. No off target effects were observed in ME06 for either target (represented as an absence of cyan and green bars in the top and bottom rows of **Figure S7F**, respectively). SM = somatomotor, ADM = auxiliary dipole method, TANS = targeted functional network stimulation.

Figure S7

